Received: 25 July 2023 | Accepted: 25 January 2024

DOI: 10.1111/1462-2920.16589

BRIEF REPORT

ENVIRONMENTAL MICROBIOLOGY Applied Microbiology International

Taxonomic and metabolic diversity of Actinomycetota isolated from faeces of a 28,000-year-old mammoth

Doris A. van Bergeijk[1,2] | **Hannah E. Augustijn**[3,4] | **Somayah S. Elsayed**[3] | **Joost Willemse**[3] | **Victor J. Carrión**[3,5,6] | **Chao Du**[3] | **Mia Urem**[3] | **Lena V. Grigoreva**[7] | **Maksim Y. Cheprasov**[7] | **Semyon Grigoriev**[7] | **Hans Jansen**[8] | **Bas Wintermans**[9] | **Andries E. Budding**[10] | **Herman P. Spaink**[3] | **Marnix H. Medema**[3,4] | **Gilles P. van Wezel**[3,6]

[1]Department of Microbiology, Immunology and Transplantation (Laboratory of Molecular Bacteriology), KU Leuven, Leuven, Belgium

[2]Center for Microbiology, VIB, Leuven, Belgium

[3]Institute of Biology, Leiden University, Leiden, The Netherlands

[4]Bioinformatics Group, Wageningen University, Wageningen, The Netherlands

[5]Department of Microbiology, University of Málaga, Málaga, Spain

[6]Department of Microbial Ecology, Netherlands Institute of Ecology, Wageningen, The Netherlands

[7]North-Eastern Federal University, Yakutsk, Russia

[8]Future Genomics, Leiden, The Netherlands

[9]Department of Medical Microbiology, Adrz Hospital, Goes, The Netherlands

[10]Inbiome, Amsterdam, Netherlands

Correspondence
Gilles P. van Wezel, Institute of Biology, Leiden University, Leiden, The Netherlands.
Email: g.wezel@biology.leidenuniv.nl

Funding information
Universiteit Leiden; European Research Council, Grant/Award Numbers: 101055020-COMMUNITY, 948770-DECIPHER

Abstract

Ancient environmental samples, including permafrost soils and frozen animal remains, represent an archive with microbial communities that have barely been explored. This yet unexplored microbial world is a genetic resource that may provide us with new evolutionary insights into recent genomic changes, as well as novel metabolic pathways and chemistry. Here, we describe Actinomycetota *Micromonospora*, *Oerskovia*, *Saccharopolyspora*, *Sanguibacter* and *Streptomyces* species were successfully revived and their genome sequences resolved. Surprisingly, the genomes of these bacteria from an ancient source show a large phylogenetic distance to known strains and harbour many novel biosynthetic gene clusters that may well represent uncharacterised biosynthetic potential. Metabolic profiles of the strains display the production of known molecules like antimycin, conglobatin and macrotetrolides, but the majority of the mass features could not be dereplicated. Our work provides insights into Actinomycetota isolated from an ancient source, yielding unexplored genomic information that is not yet present in current databases.

INTRODUCTION

Bacteria are key to life on Earth; they are major players in biogeochemical nitrogen cycling (Kuypers et al., 2018), decompose organic matter (Stursova et al., 2012), and provide eukaryotic hosts with essential nutrients and protection against biotic and abiotic stress (Mendes et al., 2013; Tremaroli & Backhed, 2012). Bacteria also produce a wide range of natural products, among them many have applications in medicine,

Doris A. van Bergeijk and Hannah E. Augustijn contributed equally to this work.

biotechnology and agriculture (Bérdy, 2005; Hutchings et al., 2019). It is predicted that we have only uncovered a small percentage of the microbial world; the majority of microorganisms resist cultivation and many bacterial taxa have hardly been explored (Lloyd et al., 2018). Moreover, scientists have so far primarily accessed easily accessible environments, while numerous bacteria exist in remote niches such as deep-sea sediments, caves and permafrost soils (Sayed et al., 2020; van Bergeijk et al., 2020). This yet unexplored microbial world likely represents an important reservoir of biological information, including novel bacterial species, microbial pathways and natural products.

In light of the limited exploration of remote environments, delving into microbial communities from ancient sources offers a unique window into the past and may teach us important lessons on the evolution of microbial and chemical diversification. Indeed, isolation and metagenome sequencing of ancient bacteria has provided important knowledge on bacterial evolution, changes in microbiome composition, ancient diseases and potential chemical novelty (D'Costa et al., 2011; Millan-Aguinaga et al., 2019; Soldatou et al., 2021; Wibowo et al., 2021). For example, large-scale de novo assembly of microbial genomes from human paleofaeces samples revealed previously undescribed gut microorganisms and a markedly higher abundance of mobile genetic elements in our ancestral gut microbiome compared to modern industrial gut microbiomes (Wibowo et al., 2021). A metagenomic survey of ancient Alaskan soil confirmed that homologues of different resistance genes existed in ancient bacteria, showing that antibiotic resistance predates the modern selective pressure of clinical antibiotic use (D'Costa et al., 2011). Furthermore, Actinomycetota isolated from 1000-year-old Arctic and Antarctic sediments showed promising bioactivity against drug-resistant pathogens, and genome mining showed low similarity to known antibiotics (Millan-Aguinaga et al., 2019; Soldatou et al., 2021). These studies illustrate how ancient sources can lead to evolutionary insights, as well as novel microorganisms and chemistry.

Furthermore, microbial communities from ancient sources may among others, be harnessed for isolation of novel bacterial species and drug discovery. Bacteria produce a wide range of natural products, including numerous bioactive molecules with applications in medicine, biotechnology and agriculture (Bérdy, 2005; Hutchings et al., 2019). Many of these metabolites are produced by members of the highly diverse phylum Actinomycetota. Their genomes typically contain many biosynthetic gene clusters (BGCs) that encode the cellular machinery for the biosynthesis of natural products, allowing them to produce an unprecedented diversity of specialised metabolites. Although many bioactive compounds produced by Actinomycetota have been identified, genomic research shows that a large part of the metabolic diversity of this phylum is still unexploited (Gavriilidou et al., 2022). The isolation of bacteria from extreme or unusual environments, such as deserts and deep-sea sediments, has been a prolific avenue for natural product discovery, leading to the identification of nearly 200 new bacterial secondary metabolites (Sayed et al., 2020). Building on this success, the exploration of ancient sources, such as permafrost soils, holds promise for uncovering unexplored Actinomycetota species and chemistry.

In this study, we aimed to isolate Actinomycetota from an ancient source to study their genomic characteristics and investigate their bioactive potential. In August 2012, an adult female woolly mammoth (*Mammuthus primigenius*) was recovered on Maly Lyakhovsky Island (74°07′ N, 140°40′ E) (Grigoriev et al., 2017; Kornienko et al., 2018), which is part of the New Siberian Islands. These islands are located between the Laptev Sea and the East Siberian Sea and contain permafrost deposits that have been preserved for more than 200,000 years (Wetterich et al., 2019). These islands are considered a time capsule to ancient biology and have been an important source of ancient animal remains, including mammoths (Nikolskiy et al., 2011). The mammoth carcass was submerged in permafrost, exposing the skull, postcranial elements and partial trunk. The lower part of the body was surrounded by almost pure ice and included the lower parts of the head, the distal portion of the trunk, chest, abdomen, front legs and distal half of the right hind leg (Goncharov et al., 2016; Grigoriev et al., 2017; Kornienko et al., 2018). The mammoth was determined to be approximately 28,500 years old and the remains contained exceptionally well-preserved soft tissues, including its intestinal tract. The skin had retained its elasticity and mummification of the carcass was minimal (Goncharov et al., 2016; Grigoriev et al., 2017; Kornienko et al., 2018).

The finding of this exceptionally well-conserved ancient specimen provided a unique opportunity to explore its ancient microbiome for Actinomycetota. Actinomycetota reproduce as exospores, which should allow their long-term survival in permafrost making it possible to isolate species from a 28,500 faecal sample (Lewin et al., 2016). In this study, we isolated Actinomycetota from this extraordinary ancient sample, compared the genomes to those of their closest modern-day neighbours, and analysed their bioactive potential. Sequencing of the six isolated Actinomycetota revealed significant phylogenetic distance to currently known strains, with yet uncharacterised biosynthetic potential.

EXPERIMENTAL PROCEDURES

Sample acquisition

In February 2014, the specimen was transported by truck to Yakutsk. Dissection of the specimen was done

in the autopsy room of the medical faculty of the University of Yakutsk. The samples for microbiological analysis were extracted from 10 to 14 March 2014, the timespan in which the remains were completely thawed. As thawing set on from the outside of the carcass and slowly proceeded inward, each day freshly thawed samples could be taken. Approached from the right side, the intestines were exposed on 13 March after carefully removing soft tissue and ribs over the previous days. A 60 cm intestinal specimen was taken out of the remains and placed on a sterile surface for further examination. No defects of the intestinal lumen were found. After inspection, two perpendicular (5 cm) incisions were made, and the intersection was folded over, exposing the intestinal very core of the lumen. Faecal samples were carefully taken from the lumen using flocked swab collecting tubes (eSwab Copan) or deposited in sterile collection tubes with disposable tweezers with minimal possible cross-contamination. Sterile examination gloves and instruments were used during the whole procedure.

Isolation of Actinomycetota

Approximately, 100 mg of faeces was aseptically placed into a sterile Eppendorf, dissolved in dH_2O, and serially diluted (10^{-1}–10^{-6}). Serial dilutions were plated onto different agar media. The media were glucose agar (GA) (Zhu et al., 2014), humic acid agar (HA) (Hayakawa & Nonomura, 1987), mannitol soya flour medium (SFM) (Kieser et al., 2000), modified Starch-Casein agar (Kuester & Williams, 1964), minimal medium without carbon sources (MM) (Kieser et al., 2000), MM + 1% glycerol (w/v) (Y), MM + 1% mannitol (w/v) (A). All media contained nystatin (50 μg/mL) and nalidixic acid (10 μg/mL) for the inhibition of fungi and Gram-negative bacteria, respectively. Plates were incubated at 30°C, 4°C and anaerobically at room temperature. Single actinomycete colonies were streaked onto SFM agar plates until pure and cryopreserved with glycerol (20%) and stored at −80°C.

Genome sequencing

Strains were cultured in TSBS (tryptic soy broth + 10% sucrose) at 30°C with 200 rpm shaking speed. Genomic DNA (gDNA) was isolated by phenol-chloroform extraction as described previously (Kieser et al., 2000) and sent to be commercially sequenced at Future Genomics Technologies, The Netherlands. Genomes were sequenced using the MinION Nanopore sequencing platform and Illumina NovaSeq6000. Hybrid assembly (both Illumina and Oxford Nanopore Technologies reads) was performed for each isolate using Unicycler (v0.4.0.7) (Wick et al., 2017). Briefly, Unicycler performs a SPAdes assembly of the Illumina reads and then scaffolds the assembly graph using long reads. Unicycler polishes its final assembly with Illumina reads and uses Pilon (Walker et al., 2014) to reduce the rate of small base-level errors.

Metagenome sequencing

The gDNA of the ice and faecal sample was isolated and sent to be commercially sequenced at Future Genomics Technologies, The Netherlands. There, they quantified the gDNA concentration using a Qubit fluorometer and TapeStation system. As the amounts of detectable gDNA were low, a QIAGEN REPLI-g kit was applied to the samples (Table S6). This successfully increased the gDNA concentration of the ice sample, whereafter sequencing was performed with the Illumina NovaSeq6000. Sequencing adapters were removed by applying the read trimming tool Trimmomatic v0.39 (Bolger et al., 2014).

Phylogenetic analysis

The initial taxonomy of the six isolates was determined using 16S rRNA sequences and BLASTN, with the highest-scoring sequencing hits reported. To determine the phylogenetic class of the isolates on a whole-genome scale, 578 Actinomycetota genome sequences have been downloaded from the PhyloPhlAn v3.0 (Asnicar et al., 2020) database, using the phylophlan_get_reference function. Next, the phylophlan_write_config_file script is employed to create a configuration file with DIAMOND as a mapping tool, MAFFT for the multiple sequence alignment, trimAl for alignment trimming and IQ-TREE for generating a phylogenetic tree. FastANI v1.32 (Jain et al., 2018) was used to calculate the relatedness of the isolates and neighbouring strains. The identities by high-scoring segment pair calculations of GGDC v3.0 were used to perform the dDDH analysis (Meier-Kolthoff et al., 2022).

Bioactive potential and comparative genome analysis

AntiSMASH v6.0 (Blin et al., 2021) was used under default settings to predict BGCs from the six isolated bacteria and their modern-day closest known neighbours. The neighbours of *Streptomyces* sp. M19 were downloaded from NCBI using accession numbers: GCA_000147815.3 (*Streptomyces violaceusniger* Tu 4113), GCA_000418455.1 (*Streptomyces rapamycinicus* NRRL 5491), GCA_002812405.1 (*Streptomyces* sp. M56) and GCA_900105695.1 (*Streptomyces melanosporofaciens*). These strains are used as input for

the pangenome graph builder tool pggb v0.4.0 (Garrison et al., 2021) using 90% sequence identity and a segment length of 10,000.

Stereomicroscopy and scanning electron microscopy

Isolates were grown for 9 days on SFM. Stereo microscopy was done using a Leica MZ16 FA microscope equipped with a Leica DFC420 C camera. Scanning electron microscopy (SEM) studies were performed using a JEOL JSM-7600F SEM (Keijser et al., 2003). Single colonies were excised from agar plates and the bottom layer of agarose was cut off to minimise the thickness of the sample. The sections were glued upon a Cryo-EM stub and the whole stub was submerged in non-boiling liquid nitrogen and frozen for 20 s. The stub was then transferred to the gatan Cryo unit, heated to −90°C for 2 min to remove any ice crystals formed during the transfer, cooled to −120°C and coated with gold/palladium (80/20) using a sputter coater. Hereafter, the samples were transferred into the microscope and kept at −120°C while imaging.

Antimicrobial activity assays

Bacillus subtilis 168, *Escherichia coli* ASD19 (Liu & Douthwaite, 2002), and *Pseudomonas aeruginosa* PA01 were used as indicator strains for antimicrobial activity and were cultured in Luria-Bertani (LB) broth at 37°C (Zhu et al., 2014). Antimicrobial activity assays were conducted in liquid and on a plate, using different methods:

Liquid-grown cultures: strains were grown in International *Streptomyces* Project 2 (ISP2) (DSMZ #987) and NMMP (Kieser et al., 2000) medium for 7 days. Wells were created in soft LB agar (1.8% w/v agar) containing one of the indicator strains pre-grown in liquid LB to exponential phase ($OD_{600} = 0.4–0.6$) by using the opposite end of the pipette tip. The wells were filled with 100 μL culture supernatant. Plates were incubated overnight at 37°C (±18 h) and the following day, the zone of inhibition was determined.

Cross-streak method: each strain was independently inoculated on nutrient agar (NA) (Difco) and ISP2 agar plates as a single streak in the centre of the plate and incubated for 7 days to allow the strains to grow and produce antibiotics. The plates were then seeded with the indicator strains pre-grown in liquid LB to exponential phase ($OD_{600} = 0.4–0.6$) by streaking perpendicular to the line of Actinomycetota growth and incubated overnight at 37°C (±18 h). The following day, the inhibition distance was determined.

Double-layer agar method: strains were manually spotted (2 μL) on MM agar plates supplemented with 0.5% mannitol and 1% glycerol (w/v) as non-repressing carbon sources, and Czapek Dox plates. After 7 days of incubation, plates were overlaid with soft LB agar (1.8% w/v agar) containing one of the indicator strains pre-grown in liquid LB to exponential phase ($OD_{600} = 0.4–0.6$) and incubated overnight at 37°C (±18 h). The following day, the zone of inhibition was determined.

Volatile assay: the antimicrobial activity of volatile compounds was assessed using a Petri dish with two equally sized compartments separated by a plastic divider, both filled with NA. Mammoth isolates were streaked on one side and plates were incubated for 7 days, after which *E. coli* or *B. subtilis* were inoculated on the other side at a concentration of 10^4 and 103 colony-forming units (cfu)/mL, respectively.

Metabolite profiling, MS/MS-based molecular networking and dereplication

Isolates M10, M15, M19 and M46 were grown as confluent lawns on NA plates for 7 days. The agar plates were cut into small pieces, soaked overnight in ethyl acetate (EtOAc) to extract the metabolites, evaporated at room temperature, and dissolved in methanol (MeOH) to a concentration of 1 mg/mL. Liquid chromatography with tandem mass spectometry (LC–MS/MS) acquisition and MS/MS-based molecular networking was performed as described previously (Van Bergeijk et al., 2022). LC-MS/MS data were deposited in the MassIVE Public GNPS data repository (MSV000093121).

Bioactivity crude extracts

The activity of the crude extracts was determined in triplicate. Indicator strains were pre-grown in liquid LB to exponential phase ($OD_{600} = 0.4–0.6$). Cultures were diluted to $OD_{600} = 0.01$ in LB and 100 μL of diluted culture was loaded into wells of a 100-well honeycomb plate. Twenty micrograms of crude extract was added to the wells. Additionally, the following controls were added: LB, bacterial dilution (growth control), bacterial cells + 6 μg ampicillin (positive control) and bacterial cells + MeOH (negative control). Subsequently, the OD_{600} was measured every 30 min for 16 h using a Bioscreen C Reader (Thermo Scientific, Breda, The Netherlands), with continuous shaking. The OD_{600} was plotted against the time.

RESULTS

Isolation of Actinomycetota from mammoth faeces

The discovery of a well-preserved mammoth on Maly Lyakhovsky Island (Grigoriev et al., 2017; Kornienko

et al., 2018) (Figure S1) provided a unique opportunity to recover ancient Actinomycetota and compare their genomes and biosynthetic potential to their modern descendants. From 10 to 14 March 2014, we joined an international team of researchers during the dissection of this extraordinary specimen. During the dissection, every day, a deeper layer of the mammoth tissue became accessible, as the specimen gradually thawed. When the thawing had proceeded far enough to explore the abdominal cavity, we found a large part of the intestines fully intact, with the omentum still attached (Figure S1). Faecal samples were carefully taken from the very core of the lumen under sterile conditions, thereby avoiding any cross-contamination (Figure S1).

A fraction of the collected faecal sample was homogenised in sterile dH_2O and plated onto various media selective for Actinomycetota, including humic acid (HA), which activates spore germination and is frequently used for the selective isolation of actinomycetes (Zhu et al., 2014). Bacterial colonies were grown on different media for phenotypic discrimination and selected based on their filamentous morphology, resulting in the isolation of six morphologically distinct strains. The majority of the strains were isolated using selective HA and/or GA plates incubated at 30°C. No filamentous bacteria were observed after anaerobic incubation. To determine the taxonomic relatedness of the isolates, full genome sequences were obtained using a combination of Nanopore and Illumina sequencing (Table S1). Comparison of the 16S rRNA sequence to those within the EzBioCloud database showed that the isolates belonged to five genera of Actinomycetota, namely *Sanguibacter* (M9), *Micromonospora* (M12), *Oerskovia* (M15), *Saccharopolyspora* (M46) and *Streptomyces* (M10 and M19), revealing that we were able to recover Actinomycetota from the 28,500 year-old-sample.

Taxonomic and phenotypic profiling of the Actinomycetota

To gain insights into the relatedness of the isolated bacteria to current known bacterial species, a maximum-likelihood tree was constructed based on whole-genome sequences of the six isolates and the whole genomes of 578 Actinomycetota representing six bacterial families and over 40 different genera using the phylogenetic profiling tool PhyloPhlAn (Figure 1). The relatedness of the isolates and neighbouring organisms was determined by calculating the average nucleotide identity (ANI) and digital DNA–DNA hybridisation (dDDH) scores in an all-to-all genome comparison, revealing the extent of genetic distinctiveness among these microbes. The ANI and dDDH scores revealed a surprisingly large phylogenetic distance between the mammoth isolates and currently known strains, with similarity scores ranging from 82% to 89% and 24% to 37%, respectively (Table S2). Of the isolates, the largest phylogenetic distance was found for *Streptomyces* sp. M19 and its closest neighbours with an ANI score <83%. These notable distances suggest that these isolates may represent novel subspecies within Actinomycetota, thereby expanding our knowledge of microbial diversity.

Taxonomic analysis revealed a substantial phylogenetic difference between the genomes of the isolates and those of their closest known neighbours, as indicated by the branch lengths (Figure 1). This was especially surprising for the *Streptomyces* isolates, which were compared to more than 300 fully annotated complete genomes. We wondered whether the low similarity was a result of the ancient origin of the strains or whether this was related to the underexplored environment from which the strains were sampled. Therefore, in addition to the comparison with phylogenetically related strains, we analysed the phylogenetic distance between other strains isolated from extreme environments and their closest neighbours found in public databases. For this, we selected two deep-sea isolates and desert isolates, and one strain isolated from the Great Salt Plains in Oklahoma (Chen et al., 2013; Cornell et al., 2018; Hohmann et al., 2009; Ma et al., 2021) (Table S3). In general, the results show higher relatedness to the closest neighbours of these strains (ANI scores >93%, compared to 82%–89% for our isolates), except for *Streptomyces* sp. SCSIO 3032 (ANI: 85.48%) and *Streptomyces thermolilacinus* SPC6 (ANI: 88.22%). It should be noted that the closest known neighbour of *S. thermolilacinus* SPC6 is an isolate from island soil, while this strain itself was isolated from a soil sample collected in the desert. Additionally, *Streptomyces* sp. SCSIO 3032 and its neighbour *Streptomyces* sp. MP131-18 both originate from deep-sea samples but from different sampling locations. Thus, we cannot exclude that the low level of similarity observed between the genomes of our strains and publicly available genomes may be due to the lack of bacteria isolated from similar environments, rather than the age of the strains themselves. Further analyses of ancient samples should shed more light on this important question.

Morphological characterisation of the isolates

To further characterise the isolated Actinomycetota and obtain a more detailed view of their morphology, the isolates were grown on SFM agar and subsequently analysed by microscopy. Stereomicroscopic analysis revealed a wide range of phenotypes (Figure 2A). *Sanguibacter* sp. M9 produced bright yellow round

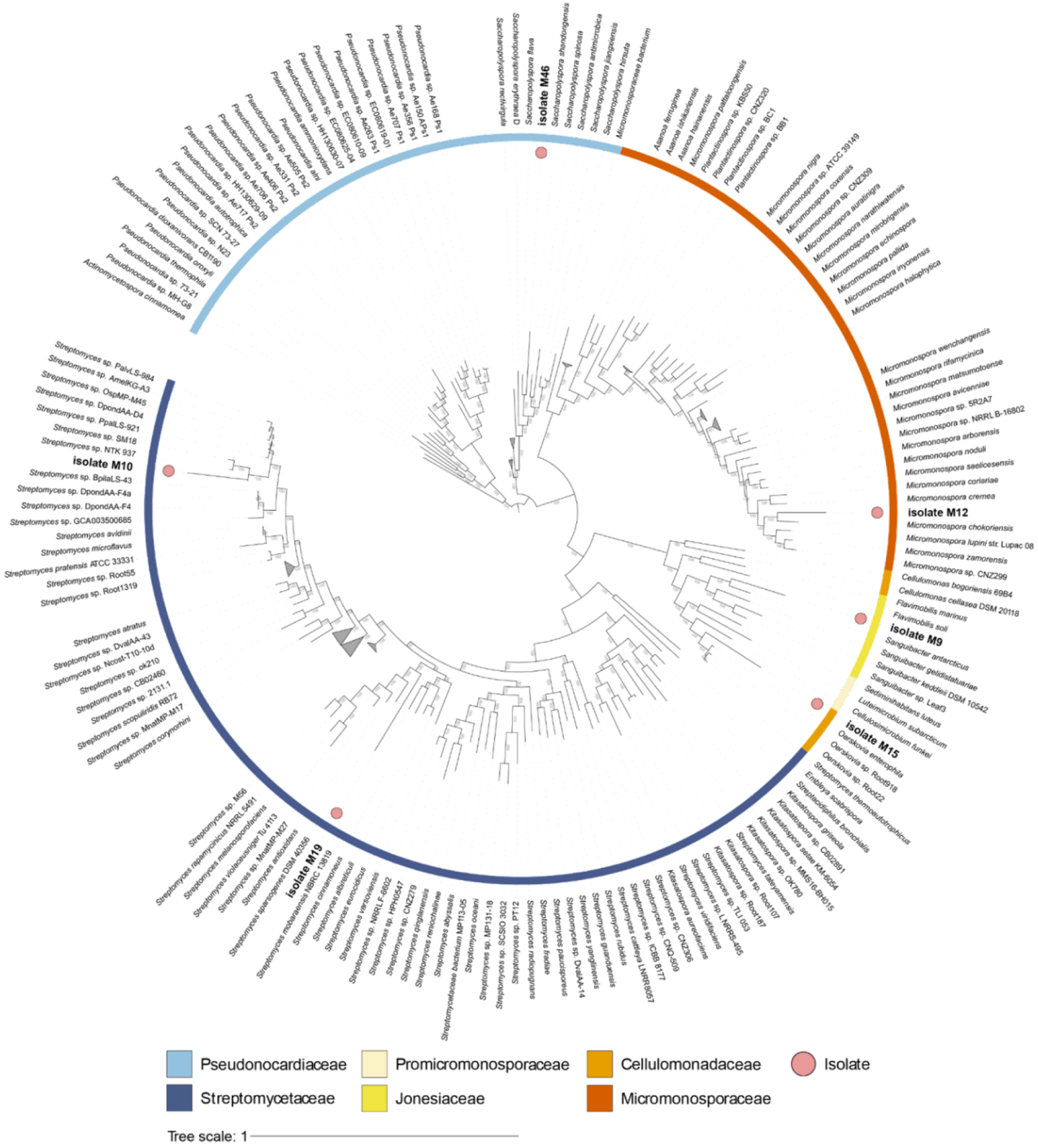

FIGURE 1 Phylogeny of whole-genome sequences of mammoth isolates and their closest known relatives. PhyloPhlAn-based maximum-likelihood tree of the six isolates compared to 578 Actinomycetota of six bacterial families (colour-coded in the outer ring), subdivided into 40 genera. The tree was rooted using *Pseudonocardia* sp. as outgroup and the numbers on the tree branches represent the bootstrap values in percentages of a total of 1000 bootstraps. Circles indicate the location of the novel isolates. The phylogenetic analysis suggests the following likely classification based on their nearest neighbours: M9, *Sanguibacter*; M12, *Micromonospora*; M15, *Oerskovia*; M10 & M19, *Streptomyces*; M46, *Saccharopolyspora*.

colonies, *Streptomyces* sp. M10 produced cream-coloured substrate mycelia, a grey aerial spore mass and a dark diffusible pigment, *Micromonospora* sp. M12 produced orange-coloured folded colonies, *Oerskovia* sp. M15 produced white colonies and *Saccharopolyspora* sp. M46 produced cream-coloured folded colonies. *Streptomyces* sp. M19 displayed a heterogeneous phenotype. When this isolate was grown on SFM agar, two colony phenotypes were observed: a fully developed phenotype, and a variant with strong

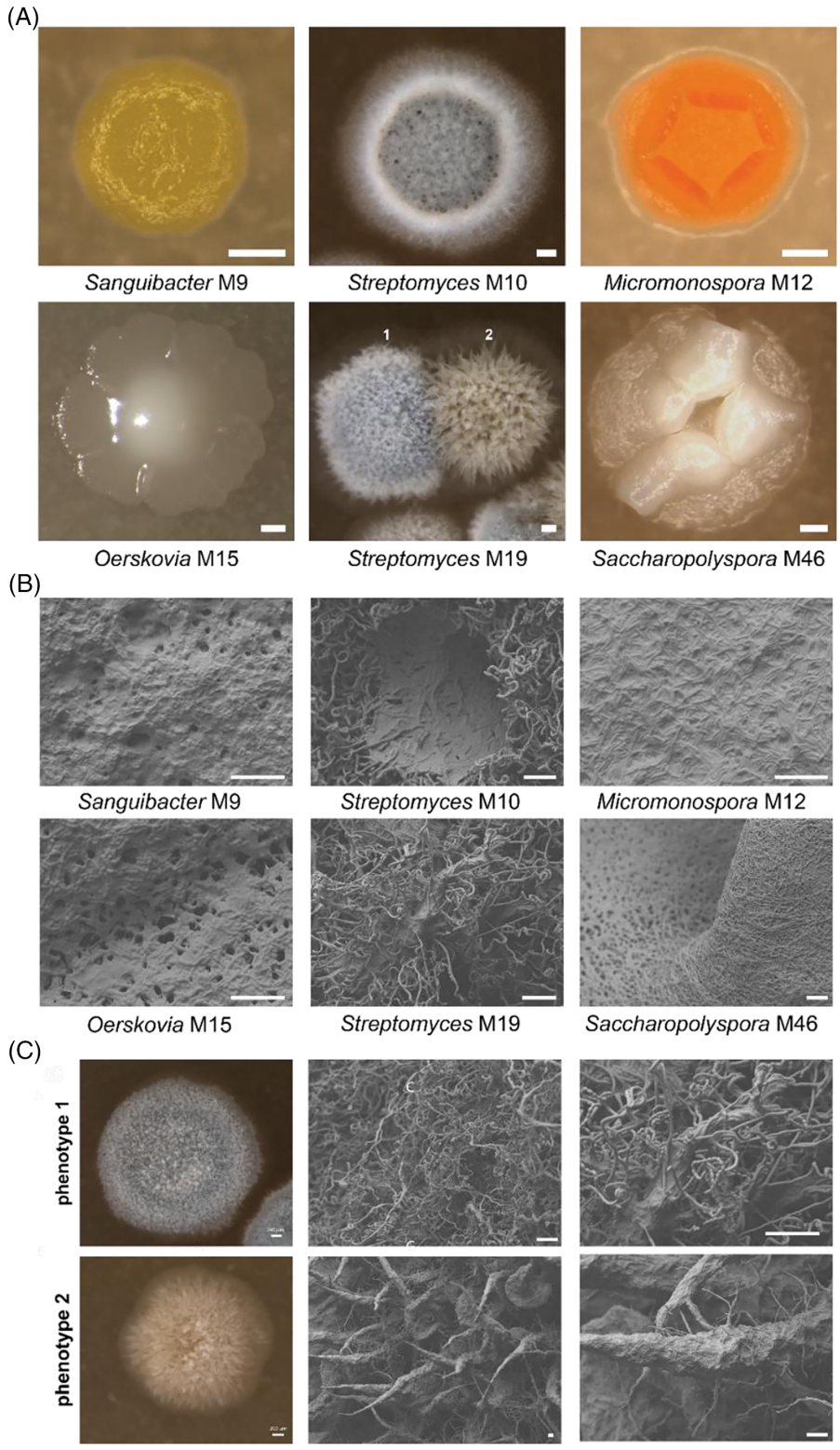

FIGURE 2 Phenotypic characterisation of Actinomycetota isolated from a faecal sample of a 28,000-year-old mammoth. Strains were grown on soya flour medium (SFM) agar plates for 9 days. (A) Stereomicrographs of isolates *Sanguibacter* sp. M9, *Streptomyces* sp. M10, *Micromonospora* sp. M12, *Oerskovia* sp. M15, *Streptomyces* sp. M19 and *Saccharopolyspora* sp. M46 (for phylogenetic analysis see Figure 1). *Streptomyces* sp. M19 showed two distinct phenotypes: fully developed colonies (1) and colonies with a bald appearance (2). Scale bar: 200 μm. (B) Scanning electron micrographs of isolates M9, M10, M12, M15, M19 and M46. Scale bar: 10 μm. (C) Scanning electron micrographs showing significant differences in morphology between the two colony phenotypes observed when *Streptomyces* sp. M19 is grown on SFM. Images of phenotype 1 show spirals of spore chains. Images of phenotype 2 show large spikes made up of hyphae and extracellular matrix. Also in the fully developed colony, such spikes can be found but in low frequency. The 16S rRNA sequencing strongly suggests that these morphological variants are phenotypes of *Streptomyces* sp. M19. Scale bar: 10 μm.

yellow pigmentation, sparse aerial mycelia and lack of spores. Morphological heterogeneity was also observed within single colonies (Figure S2), suggesting a high tendency to genetic heterogeneity (Zhang et al., 2020). Sequencing of the 16S rRNA strongly suggests that all morphological variants were indeed phenotypes of the same strain.

To study the morphology of the isolates in high resolution and obtain more insights into the heterogeneous morphology of *Streptomyces* sp. M19, colonies were subjected to SEM (Figure 2B). Colonies of *Streptomyces* sp. M10 produced hairy spores, whereby the aerial mycelium consisted of both smooth and hairy hyphae, with dark-pigmented droplets on top of the colonies. *Saccharopolyspora* sp. M46 colonies consisted of a thick layer of interwoven mycelium made up of hyphae and extracellular matrix. SEM studies of the two distinct phenotypes of *Streptomyces* sp. M19 revealed spiral spore chains in one variant (phenotype 1), while we failed to identify spores in the other (phenotype 2) (Figure 2C). Instead, the non-sporulating colonies produced large spikes made up of hyphae embedded in an extracellular matrix. These spikes could also be found in the fully developed colony but in low abundance. Colonies of isolates *Sanguibacter* sp. M9, *Micromonospora* sp. M12 and *Oerskovia* sp. M15 were covered by an extracellular matrix and could therefore not be further characterised by SEM.

Biosynthetic potential of the isolated bacteria

Next, we predicted the presence of BGCs for natural products in the genomes of the isolates, to assess their relatedness to BGCs that are currently available in the databases. For this, the genome sequences were analysed using antiSMASH (Blin et al., 2021). This identified a total of 179 putative BGCs, namely four in *Oerskovia* sp. M15, six in *Sanguibacter* sp. M9, 19 in *Saccharopolyspora* sp. M46, 23 in *Micromonospora* sp. M12, 31 in *Streptomyces* sp. M10 and 34 in *Streptomyces* sp. M19 (Figure 3A). Over 70% of the total BGCs shared less than 50% KnownClusterBlast similarity to BGCs within the MiBIG database, with 23% showing no significant similarity to any known BGC. This amounts to a similar amount of biosynthetic novelty compared to many genomes from contemporary strains (Table S4).

The genome sequence of *Streptomyces* sp. M19 showed the largest distance in terms of ANI scores to its nearest neighbours. We therefore subjected the strain to detailed analysis of its biosynthetic potential, to obtain insights into the chemical diversity of its specialised metabolites. *Streptomyces* sp. M19 is predicted to have seven closest neighbours (Table S3). Out of these seven, we selected four strains with the highest quality assemblies for comparative genome analysis, namely *S. violaceusniger* Tu 4113, *S. rapamycinicus* NRRL 5491 and *Streptomyces* sp. M56, *S. melanosporofaciens* (Figure 3B). The M19 genome had a slightly lower number of predicted BGCs (34) than these nearest neighbours (47–54 BGCs). Surprisingly, *Streptomyces* sp. M19 only shares two BGCs with its nearest neighbours, namely for desferrioxamine and ectoine. Additionally, the M19 genome encodes many non-ribosomal peptide synthetases and polyketide synthases (PKSs), and also has BGCs for butyrolactones, unusual polyketides/fatty acids (linked to a heterocyst glycolipid synthase-like PKS, and another unusual type of ketosynthase related to those found in ladderane lipid biosynthetic pathways) a likely lasso peptide, an aryl polyene and an aminoglycoside/aminocyclitol; none of these natural product classes could be found in modern nearest neighbours. Comparative genomic analysis of *Streptomyces* sp. M19 and its four neighbours display a low similarity score of approximately 82% and only a few corresponding BGCs (Figure S3).

Antibiotic activity and bioactive metabolites produced by the mammoth isolates

Next, the antibiotic-producing potential of the strains was assessed under six different culturing conditions. These were four agar-based media, namely the nutrient-rich NA and ISP2 and the nutrient-poor Czapek Dox and MM supplemented with mannitol and glycerol, and the liquid media versions of ISP2 and MM. We used the Gram-positive *B. subtilis* 168 and the Gram-negative *E. coli* ASD19 and *P. aeruginosa* PA01 as indicator strains. Different types of growth inhibition were observed, namely complete inhibition, a strong reduction in the number of cfu, and impaired growth (Figure 4). Under the conditions tested, the isolates displayed the strongest antibacterial activity when grown on NA. Therefore, further metabolic analysis was done on samples isolated from NA-grown cultures.

Besides soluble natural products, volatile organic compounds (VOCs) may have antibacterial activity (Avalos et al., 2018, 2020). To investigate whether (some of) the antimicrobial activity may have been due to the production of antibacterial VOCs, the isolates were grown on plates where the Actinomycetota were separated from the indicator strains by an impermeable polystyrene divider. Interestingly, the growth of *E. coli* was completely inhibited by VOCs produced by isolates of *Streptomyces* sp. M10, *Streptomyces* sp. M19 and *Saccharopolyspora* sp. M46 (Figure S4). While *Micromonospora* sp. M12 did not display antibacterial activity in the bioactivity assay described above, it partially inhibited the growth of *E. coli* in the volatile assay.

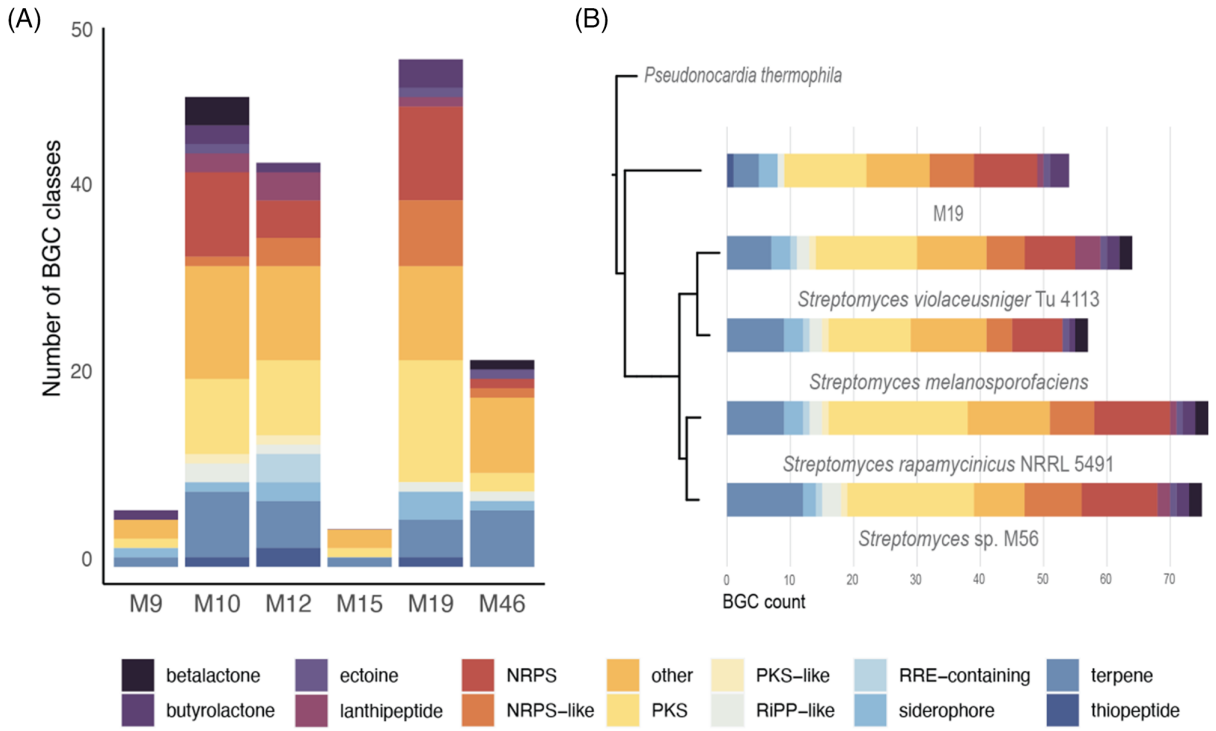

FIGURE 3 Classification of biosynthetic gene clusters (BGCs) predicted in the Actinomycetota genomes. (A) BGC classes for each isolate predicted with antiSMASH v6.0. Known types of BGCs representing <1% of all BGCs were grouped into the "other" category. The large number of BGCs in *Streptomyces* spp. M10 and M19, *Micromonospora* sp. M12 and *Saccharopolyspora* sp. M46 is particularly noteworthy. (B) Overview of all predicted BGC classes for isolate M19 and its closest neighbours *Streptomyces violaceusniger* Tu 4113, *Streptomyces rapamycinicus* NRRL 5491, *Streptomyces* sp. M56 and *Streptomyces melanosporofaciens*. The comparison shows that only two BGCs are shared between all three isolates, namely BGCs for desferrioxamine and for ectoine. Moreover, the genome of *Streptomyces* sp. M19 contains a greater variety of BGC classes, with a surprisingly high proportion of non-ribosomal peptide synthetases (NRPS) BGCs. PKS, polyketide synthases. RiPPs, ribosomally synthesized and post-translationally modified peptides. RRE, RiPP recognition element.

	Bacillus subtilis						*Escherichia coli*						*Pseudomonas aeruginosa*					
	1	2	3	4	5	6	1	2	3	4	5	6	1	2	3	4	5	6
M9	0	0	0	0	0	0	0	0	0	0	0	0	0	0	0	0	0	0%
M10	0.7	1.1	0	0	0.6	1.7	0	0	0	0	0	2.2	0	0	0	0	0	RG
M12	0.6	0.6	0	0	0	0	0.6	0.5	0	0	0	0	0	0	0	0	0	0%
M15	0	0	0	0	0	0.6	0	0	0	0	0	0	0	0	0	0	0	0%
M19	1.9	0	1.8	1.7	0.6	1.1	0	0	0	0.9	0	3.2	0	0	0	0	0	0%
M46	0	0	0	0	0	3.6	0	0	0	0	0	3.3	0	0	0	0	0	RG

FIGURE 4 Antimicrobial activity of the Actinomycetota isolates. After 7 days of growth, the antimicrobial activity of the mammoth isolates was assessed against different indicator strains using different growth media and methods: 1 = minimal medium (MM), soft agar overlay; 2 = Czapek Dox, soft agar overlay; 3 = liquid culture International *Streptomyces* Project 2 (ISP2); 4 = liquid culture MM; 5 = ISP2, cross-streak, 6 = nutrient agar (NA), cross-streak. The zone of inhibition (cm) is indicated for each isolate and related to a colour scale ($n = 3$). Most activity was observed in the cross-streak assay on NA. RG, reduced growth.

None of the strains produced VOCs that could inhibit the growth of *B. subtilis*. These data indicate that the observed antibacterial activity of strains M10, M19 and M46 against *E. coli* was at least in part caused by VOCs, while the bioactivity of isolates M10, M15, M19 and M46 against *B. subtilis* was solely caused by the production of soluble antibiotics.

To gain more insights into the soluble antibiotics produced by isolates of *Oerskovia* sp. M15, *Streptomyces* sp. M10, *Streptomyces* sp. M19 and *Saccharopolyspora* sp. M46, the strains were streaked on NA plates and grown for 7 days. Metabolites were extracted using EtOAc and tested for bioactivity against the different indicator strains. The crude extracts of *Streptomyces*

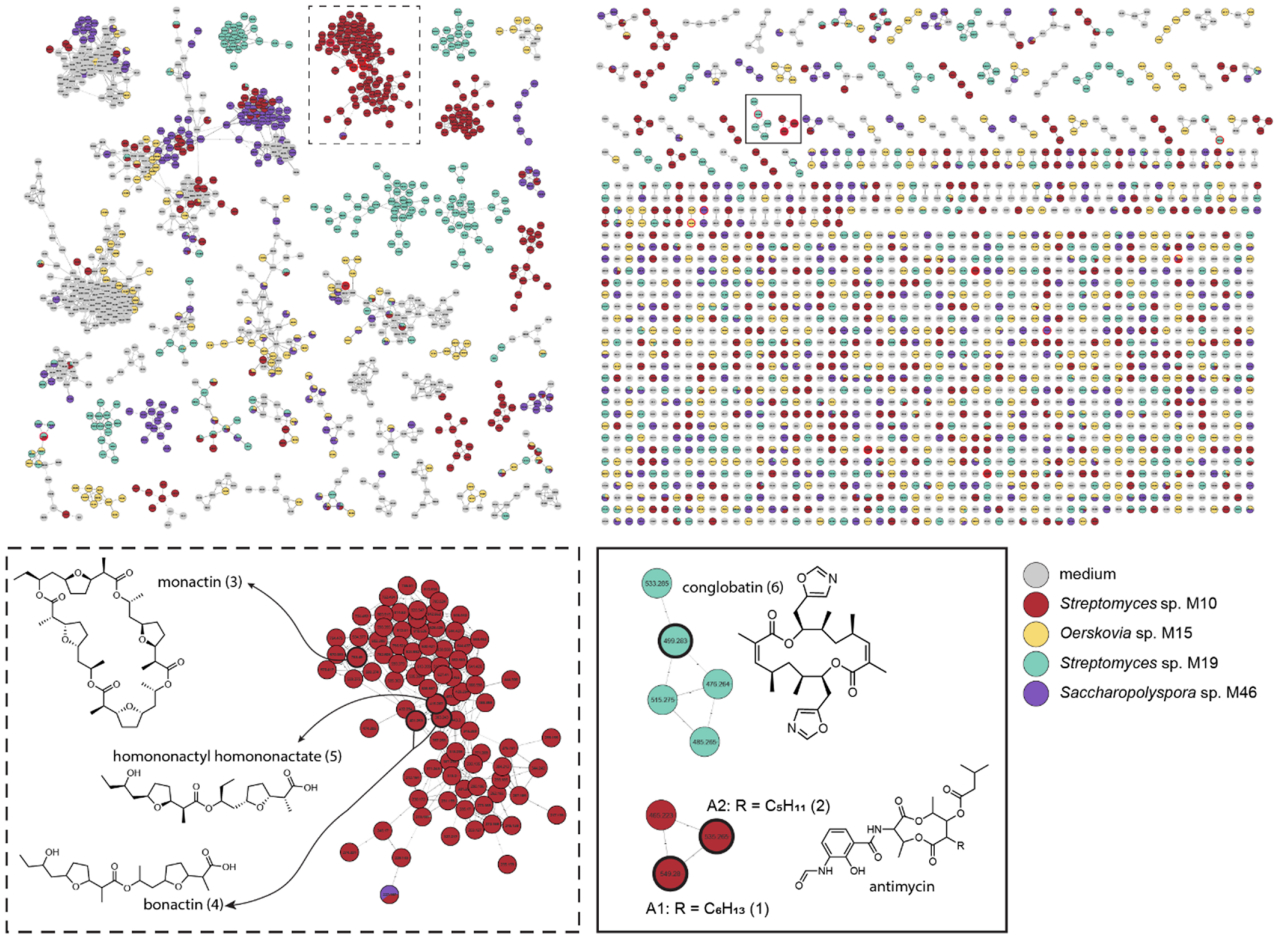

FIGURE 5 Molecular network of the ions detected in the crude extracts of the isolates and dereplication of bioactive compounds. A pie chart was mapped to the nodes which represents the abundance of each *m/z* value in the crude extracts of the different bioactive isolates (M10, M15, M19 and M46). Grey nodes indicate mass features that were also present in the medium blank. Nodes highlighted represent dereplicated known bioactive metabolites. Annotation was confirmed by manually checking the fragmentation data and the presence of the responsible biosynthetic gene clusters in the genome. The isolates were grown for 7 days on nutrient agar agar plates ($n = 3$).

sp. M10 and M19 showed activity against *B. subtilis*, while *E. coli* and *P. aeruginosa* were not inhibited (Figure S5). MS/MS data were analysed using Global Natural Products Social Molecular Networking (GNPS) (Wang et al., 2016), resulting in a molecular network containing 2886 nodes clustered in 223 spectral families (Figure 5). The highest number of unique nodes (491) were attributed to isolate M10, while the lowest number (280) was attributed to isolate M46. Fourty-four nodes were unique to *Streptomyces* isolates M10 and M19. The molecular network also revealed several spectral families (≥3 nodes) that were unique to each of the isolates and did not include features present in the medium blank; 11 were found in *Streptomyces* sp. M10, 8 in *Oerskovia* sp. M15, 10 in *Streptomyces* sp. M19 and 2 in *Saccharopolyspora* sp. M46. Dereplication based on matching MS/MS spectra against the GNPS spectral library annotated 247 nodes (8.5% of 2886), the majority of which was also present in the medium blank. Eighteen features were annotated that were unique to the isolated bacterial strains (Table S5), including several known bioactive metabolites: antimycin A1 (**1**), antimycin A2 (**2**), monactin (**3**) and bonactin (**4**) and homononactyl homononactate (**5**) in the extracts of M10, and conglobatin (**6**) in the extracts of M19 (Figure 5). The annotation of these metabolites was checked manually using the fragmentation data. To further validate these findings, we analysed the KnownClusterBlast output of antiSMASH for the presence of the responsible BGCs. In the genome of M10, antiSMASH identified an antimycin BGC and a BGC with a 75% KnownClusterBlast similarity score to the macrotetrolide BGC of nonactin (MIBiG cluster BGC0000243). This similarity implies that M10 could potentially synthesise compounds similar to bonactin and monactin, which are known products of the nonactin cluster. The macrotetrolide-associated BGC from strain M10 lacks three genes compared to the reference BGC, two encoding hypothetical proteins and one encoding an inositol

monophosphatase-like enzyme. M19 harbours a BGC with a low (36%) similarity score to the conglobatin BGC (Figure S6). Although the overall match for this cluster is lower, we could detect homologues of all known core conglobatin genes (*congA-E*) with the same domain architecture as in the reference BGC. Taken together, the isolates produced some known bioactive molecules, but the majority of the mass features could not be dereplicated, suggesting the production of novel chemistry.

DISCUSSION

A huge proportion of the bacterial world remains uncharacterised, representing a potential reservoir of biological information and new chemistry, which may have implications for future drug discovery (Lloyd et al., 2018; Sayed et al., 2020; Sunagawa et al., 2015). Metagenome sequencing, varying culturing techniques and isolation of bacteria from rare environments are gradually revealing part of this microbial dark matter, and ancient samples offer an underexplored resource (D'Costa et al., 2011; Wibowo et al., 2021). In this study, we present Actinomycetota isolated from faeces from the intestinal tract of an exceptionally well-preserved 28,000-year-old mammoth (Grigoriev et al., 2017). Genome sequencing showed that these Actinomycetota belonged to the well-studied genus *Streptomyces* and the underexplored genera *Sanguibacter*, *Micromonospora*, *Oerskovia* and *Saccharopolyspora*. Genomic analysis of the strains revealed a large phylogenetic distance to currently known strains and substantial uncharacterised biosynthetic potential, highlighting the significance of exploring such environments.

In contrast to previous metagenome-based studies that demonstrated the presence of Actinomycetota reads in different tissues of mammoth remains (Ferrari et al., 2018), our approach involved isolating and growing the strains, minimising the risk of misassembling the (damaged) DNA and enabling a more accurate investigation of their genomic content. Ancient DNA is more difficult to isolate as it is often fragmented and available in limited amounts (Dabney et al., 2013). This is reflected in the metagenome we obtained, whereby only low concentrations of DNA could be isolated. As a result, only a fraction of the complete genomic diversity could be analysed. The isolation of Actinomycetota allows a more in-depth exploration of their functional role and potential. Taxonomic analysis revealed a substantial phylogenetic difference between the isolates and their closest known neighbours, strongly suggesting that these isolates represent novel species. The low similarity to known strains may be attributed to the limited number of publicly available complete genomes for underexplored taxa such as *Oerskovia*, *Sanguibacter* and *Saccharopolyspora*, with three, four and eight available complete genome sequences, respectively, as compared to 323 complete *Streptomyces* genomes. Nevertheless, even within the well-studied genus *Streptomyces*, our isolates exhibit low similarity scores, emphasising the uniqueness of their genomic makeup despite the availability of numerous genomes for comparison. This distinctiveness was further highlighted in our comparative genome analyses between isolate *Streptomyces* sp. M19 and its taxonomic neighbours in publicly available sequence data. This analysis revealed a shared conserved internal region and a less conserved region near the ends of the chromosome, holding high numbers of unique and uncharacterised BGCs. This is consistent with results from previous studies showing that common BGCs are often located in the internal regions of the chromosome, while more unique genes are located towards the subtelomeric regions (Ikeda et al., 2003; Letzel et al., 2017; van Bergeijk et al., 2020). Surprisingly, only two BGCs, for the desferrioxamine and ectoine pathways, were shared between isolate *Streptomyces* sp. M19 and its neighbours. These specialised metabolites play an important role in the survival and their BGCs are well-conserved (Czech et al., 2018; van Bergeijk et al., 2020). The low overlap between the biosynthetic potential of *Streptomyces* sp. M19 and its nearest neighbours is unexpected as phylogeny is an important indicator of BGC distribution (Belknap et al., 2020; Ziemert et al., 2014). In addition to its biosynthetic diversity, *Streptomyces* sp. M19 also exhibited high morphological heterogeneity within single colonies, with two distinct phenotypes based on extracellular matrix production and the presence/absence of spore chains. This could point to genetic heterogeneity, impacting environmental adaptation, bacterial fitness and metabolite production (Zhang et al., 2020). Comparison of these phenotypes can provide insights into how morphology plays a role in the ecology and evolutionary strategies of Streptomyces. Together, these results underline the opportunities offered in terms of the biosynthetic potential of bacteria isolated from underexplored environments. The majority of the isolates displayed bioactivity against one of the tested indicator strains, both through the production of volatile and non-volatile compounds. The antibacterial activity against Gram-positive bacteria by *Oerskovia* sp. M15 is noteworthy, as antibacterial activity has not been reported previously for members of this genus. While four potential BGCs were identified in the genome sequence of M15, with three having similarity scores below 12%, the crude extracts did not show any activity, and chemical dereplication did not give any hits with known bioactive compounds. The identification of the metabolite and BGC responsible for the observed bioactivity of *Oerskovia* sp. M15 will be the focus of future investigations.

Several known natural products were annotated in the bioactive extracts of *Streptomyces* isolates M10 and M19 using the GNPS platform, including antimycin and monactin in the extracts of M10 and conglobatin in the extracts of M19. This was supported by the detection of their BGCs by antiSMASH. Interestingly, antimycin- and conglobatin-related molecules were also detected in the crude extracts of polar Actinomycetota isolated from ancient sediment cores (Soldatou et al., 2021). An evolutionary path of the antimycin BGC has been proposed in which the BGC form possessing both the *antP* and *antQ* gene is appointed as the ancestor of other antimycin BGCs (Joynt & Seipke, 2018). Therefore, it is not surprising that our detected ancient BGC is the ancestral form antimycin cluster. Additionally, analysis of the biogeographical and phylogenetic distribution of the antimycin BGC has revealed that this BGC is widespread among *Streptomyces* spp. globally (Joynt & Seipke, 2018). The molecular network also revealed several spectral families unique to each of the isolated Actinomycetota that could not be dereplicated, which may represent novel chemistry, especially for the underexplored genera *Saccharopolyspora* and *Oerskovia*. Using the dereplication tool of GNPS, which compares MS2 spectra to a library of MS/MS spectra generated from structurally characterised metabolites, only 8.5% of the chemical features could be annotated. Indeed, most of the chemical data generated by mass spectrometry remains uncharacterised (da Silva et al., 2015), limiting the interpretation of metabolomics data.

Ancient samples allow a glimpse into the past and may provide evolutionary insights. The substantial differences that we observed between the isolates and their closest known relatives raised the question whether this could be related to the age of the faecal sample. 0.285 million years on a scale of 2700 million years reflects only a fraction of actinobacterial evolution, but theoretically, 10%–20% ANI variation could be obtained within this time frame. However, the analysis of evolutionary differences was complicated by the large phylogenetic distance between the isolates and their known relatives. For better comparison, genome sequences of more closely related strains are required; however, it is yet not known if such strains can be found in the available strain collections.

As our work relates to ancient microbes, it is important to provide insights into the certainty of the origin of the samples. During sample retrieval, we took maximum care to ensure that the bacteria truly originated from the mammoth faeces; this included opening the intestines under sterile conditions, obtaining a sample from a clean part of the intestinal lumen, and above all extracting a pristine sample from the very core of the faecal sample. We also attempted to use metagenome analysis to see if we could retrace the bacterial genome sequences in the intestinal metagenome and not in the surrounding ice. Previous studies on a mammoth microbiome showed that it is extremely difficult to get data of sufficient quality to ascertain the origin of microbes (Ferrari et al., 2018), and indeed we ran into similar issues, and the approach was abandoned. Finally, it is relevant to note that there are no records of scientists at our institute having previously worked with strains of the genera *Oerskovia*, *Sanguibacter* or *Saccharopolyspora*, nor are these known as common contaminants, which minimises the chance of laboratory contamination.

Much interest has been directed towards the presence of antibiotic-producing Actinomycetota in the mammalian microbiome as this could point towards a protective role against infection by pathogens (Donia et al., 2014; Zipperer et al., 2016). We were excited to be able to isolate six Actinomycetota from the faecal sample. While we do appreciate that this may seem like a low number, filamentous Actinomycetota represent only a very minor fraction of the mammalian gut and it is unknown how well spores survive such a long period of time. Antibiotic-producing Actinomycetota have been isolated from the faeces of a variety of mammals (Jiang et al., 2013; Liu et al., 2014; Ma et al., 2017) and studies analysing the microbiome composition of elephants, the closest living relative to mammoths, report the presence of Actinomycetota reads in low abundance, including *Streptomyces*, *Sanguibacter*, *Micromonospora* and *Saccharopolyspora*, but not *Oerskovia* (Budd et al., 2020; Keady et al., 2021; Zhang et al., 2019). Additionally, species of *Streptomyces* and *Micromonospora* have been isolated from the faeces of elephants (Jiang et al., 2013; Li et al., 2018). Unfortunately, these isolates have not been sequenced and could not be compared to the bacteria isolated in this study. Alternatively, the isolated Actinomycetota may not have been commensal to the mammoth gut but instead may have been obtained as part of digested plant material.

In summary, Actinomycetota were isolated from a unique ancient mammoth stool sample. The considerable phylogenetic distance between the isolates and their closest taxonomic neighbours as well as their high percentage of uncharacterised biosynthetic potential, even in the representatives of the well-studied genus *Streptomyces*, illustrate that we have by no means captured all microbial diversity. This underlines the opportunities offered in terms of the biosynthetic potential of bacteria isolated from ancient sources and highlights the importance of collecting microbial data from these environments. Continuing to map these microbial communities may provide a unique glance into microbial history.

AUTHOR CONTRIBUTIONS

Gilles P. van Wezel: Writing – original draft; funding acquisition; supervision; writing – review and editing; conceptualization; resources; project administration. **Doris A. van Bergeijk:** Conceptualization; investigation;

methodology; validation; writing - original draft; writing – review and editing; formal analysis; data curation; visualization. **Hannah E. Augustijn:** Investigation; writing – original draft; methodology; writing – review and editing; software; data curation. **Somayah S. Elsayed:** Investigation; writing – review and editing; writing – original draft; methodology; formal analysis; supervision; data curation. **Joost Willemse:** Visualization; methodology; writing – review and editing; supervision; investigation. **Victor J. Carrión:** Investigation; methodology; writing – review and editing; formal analysis. **Chao Du:** Investigation; methodology; writing – review and editing; data curation; supervision. **Mia Urem:** Investigation; writing – review and editing; methodology; formal analysis. **Lena V. Grigoreva:** Investigation; methodology; writing – review and editing; supervision; resources. **Maksim Y. Cheprasov:** Investigation; writing – review and editing; resources; formal analysis. **Semyon Grigoriev:** Investigation; formal analysis; writing – review and editing; methodology. **Hans Jansen:** Investigation; validation; methodology; formal analysis; writing – review and editing. **Bas Wintermans:** Writing – review and editing; investigation; validation. **Andries E. Budding:** Writing – review and editing; supervision; formal analysis; methodology; writing – original draft; investigation; conceptualization. **Herman P. Spaink:** Writing – original draft; supervision; formal analysis; writing – review and editing. **Marnix H. Medema:** Writing – original draft; funding acquisition; supervision; conceptualization; writing – review and editing; resources; project administration.

ACKNOWLEDGEMENTS

We are grateful to Christina Vandenbroucke-Grauls for stimulating discussions. All authors acknowledge the support from their respective research institutes. The work was supported by the European Union via ERC Starting Grant 948770-DECIPHER to Marnix H. Medema and ERC Advanced Grant 101055020-COMMUNITY to Gilles P. van Wezel and by the profile area antibiotics at Leiden University to Gilles P. van Wezel.

CONFLICT OF INTEREST STATEMENT

The authors declare no competing interests.

DATA AVAILABILITY STATEMENT

The data that support the findings of this study are openly available in the GNPS database at https://gnps.ucsd.edu/ProteoSAFe/status.jsp?task=e160b564fc7e48e6b82394991bfd79be. The genomes are available under BioProject PRJNA838256.

ORCID

Gilles P. van Wezel https://orcid.org/0000-0003-0341-1561

REFERENCES

Asnicar, F., Thomas, A.M., Beghini, F., Mengoni, C., Manara, S., Manghi, P. et al. (2020) Precise phylogenetic analysis of microbial isolates and genomes from metagenomes using PhyloPhlAn 3.0. *Nature Communications*, 11, 2500.

Avalos, M., Garbeva, P., Raaijmakers, J.M. & van Wezel, G.P. (2020) Production of ammonia as a low-cost and long-distance antibiotic strategy by *Streptomyces* species. *The ISME Journal*, 14, 569–583.

Avalos, M., van Wezel, G.P., Raaijmakers, J.M. & Garbeva, P. (2018) Healthy scents: microbial volatiles as new frontier in antibiotic research? *Current Opinion in Microbiology*, 45, 84–91.

Belknap, K.C., Park, C.J., Barth, B.M. & Andam, C.P. (2020) Genome mining of biosynthetic and chemotherapeutic gene clusters in *Streptomyces* bacteria. *Scientific Reports*, 10, 2003.

Bérdy, J. (2005) Bioactive microbial metabolites. *Journal of Antibiotics (Tokyo)*, 58, 1–26.

Blin, K., Shaw, S., Kloosterman, A.M., Charlop-Powers, Z., van Wezel, G.P., Medema, M.H. et al. (2021) antiSMASH 6.0: improving cluster detection and comparison capabilities. *Nucleic Acids Research*, 49, W29–W35.

Bolger, A.M., Lohse, M. & Usadel, B. (2014) Trimmomatic: a flexible trimmer for Illumina sequence data. *Bioinformatics*, 30, 2114–2120.

Budd, K., Gunn, J.C., Finch, T., Klymus, K., Sitati, N. & Eggert, L.S. (2020) Effects of diet, habitat, and phylogeny on the fecal microbiome of wild African savanna (*Loxodonta africana*) and forest elephants (*L. cyclotis*). *Ecology and Evolution*, 10, 5637–5650.

Chen, X., Zhang, B., Zhang, W., Wu, X., Zhang, M., Chen, T. et al. (2013) Genome sequence of *Streptomyces violaceusniger* strain SPC6, a halotolerant Streptomycete that exhibits rapid growth and development. *Genome Announcements*, 1, e00494-13.

Cornell, C.R., Marasini, D. & Fakhr, M.K. (2018) Draft genome sequences of megaplasmid-bearing *Streptomyces* sp. strains BF-3 and 4F, isolated from the great Salt Plains of Oklahoma. *Genome Announcements*, 6, e00208-18.

Czech, L., Hermann, L., Stoveken, N., Richter, A.A., Hoppner, A., Smits, S.H.J. et al. (2018) Role of the extremolytes ectoine and hydroxyectoine as stress protectants and nutrients: genetics, phylogenomics, biochemistry, and structural analysis. *Genes*, 9, 177.

da Silva, R.R., Dorrestein, P.C. & Quinn, R.A. (2015) Illuminating the dark matter in metabolomics. *Proceedings of the National Academy of Sciences of the United States of America*, 112, 12549–12550.

Dabney, J., Meyer, M. & Paabo, S. (2013) Ancient DNA damage. *Cold Spring Harbor Perspectives in Biology*, 5, a012567.

D'Costa, V.M., King, C.E., Kalan, L., Morar, M., Sung, W.W., Schwarz, C. et al. (2011) Antibiotic resistance is ancient. *Nature*, 477, 457–461.

Donia, M.S., Cimermancic, P., Schulze, C.J., Wieland Brown, L.C., Martin, J., Mitreva, M. et al. (2014) A systematic analysis of biosynthetic gene clusters in the human microbiome reveals a common family of antibiotics. *Cell*, 158, 1402–1414.

Ferrari, G., Lischer, H.E.L., Neukamm, J., Rayo, E., Borel, N., Pospischil, A. et al. (2018) Assessing metagenomic signals recovered from Lyuba, a 42,000-year-old permafrost-preserved woolly mammoth calf. *Genes*, 9, 436.

Garrison, E., Heumos, S., Guarracino, A. & Gao, Y. (2021) pggb: the PanGenome Graph Builder.

Gavriilidou, A., Kautsar, S.A., Zaburannyi, N., Krug, D., Müller, R., Medema, M.H. et al. (2022) Compendium of specialized metabolite biosynthetic diversity encoded in bacterial genomes. *Nature Microbiology*, 7, 726–735.

Goncharov, A., Grigorjev, S., Karaseva, A., Kolodzhieva, V., Azarov, D., Akhremenko, Y. et al. (2016) Draft genome sequence of *Enterococcus faecium* strain 58m, isolated from

intestinal tract content of a woolly mammoth, *Mammuthus primigenius*. *Genome Announcements*, 4, e01706–e01715.

Grigoriev, S.E., Fisher, D.C., Obadă, T., Shirley, E.A., Rountrey, A.N., Savvinov, G.N. et al. (2017) A woolly mammoth (*Mammuthus primigenius*) carcass from Maly Lyakhovsky Island (New Siberian Islands, Russian Federation). *Quaternary International*, 445, 89–103.

Hayakawa, M. & Nonomura, H. (1987) Humic acid-vitamin agar, a new medium for the selective isolation of soil actinomycetes. *Journal of Fermentation Technology*, 65, 501–509.

Hohmann, C., Schneider, K., Bruntner, C., Irran, E., Nicholson, G., Bull, A.T. et al. (2009) Caboxamycin, a new antibiotic of the benzoxazole family produced by the deep-sea strain *Streptomyces* sp. NTK 937. *Journal of Antibiotics (Tokyo)*, 62, 99–104.

Hutchings, M.I., Truman, A.W. & Wilkinson, B. (2019) Antibiotics: past, present and future. *Current Opinion in Microbiology*, 51, 72–80.

Ikeda, H., Ishikawa, J., Hanamoto, A., Shinose, M., Kikuchi, H., Shiba, T. et al. (2003) Complete genome sequence and comparative analysis of the industrial microorganism *Streptomyces avermitilis*. *Nature Biotechnology*, 21, 526–531.

Jain, C., Rodriguez, R.L., Phillippy, A.M., Konstantinidis, K.T. & Aluru, S. (2018) High throughput ANI analysis of 90K prokaryotic genomes reveals clear species boundaries. *Nature Communications*, 9, 5114.

Jiang, Y., Han, L., Chen, X., Yin, M., Zheng, D., Wang, Y. et al. (2013) Diversity and bioactivity of cultivable animal fecal Actinobacteria. *Advances in Microbiology*, 3, 1–13.

Joynt, R. & Seipke, R.F. (2018) A phylogenetic and evolutionary analysis of antimycin biosynthesis. *Microbiology*, 164, 28–39.

Keady, M.M., Prado, N., Lim, H.C., Brown, J., Paris, S. & Muletz-Wolz, C.R. (2021) Clinical health issues, reproductive hormones, and metabolic hormones associated with gut microbiome structure in African and Asian elephants. *Animal Microbiome*, 3, 85.

Keijser, B.J., Noens, E.E., Kraal, B., Koerten, H.K. & van Wezel, G.P. (2003) The *Streptomyces coelicolor ssgB* gene is required for early stages of sporulation. *FEMS Microbiology Letters*, 225, 59–67.

Kieser, T., Bibb, M.J., Buttner, M.J., Chater, K.F. & Hopwood, D.A. (2000) *Practical Streptomyces genetics*. Norwich: John Innes Foundation.

Kornienko, I.V., Faleeva, T.G., Oreshkova, N.V., Grigoriev, S.E., Grigoreva, L.V., Simonov, E.P. et al. (2018) Complete mitochondrial genome of a woolly mammoth (*Mammuthus primigenius*) from Maly Lyakhovsky Island (New Siberian Islands, Russia) and its phylogenetic assessment. *Mitochondrial DNA Part B Resources*, 3, 596–598.

Kuester, E. & Williams, S.T. (1964) Selection of media for isolation of Streptomycetes. *Nature*, 202, 928–929.

Kuypers, M.M.M., Marchant, H.K. & Kartal, B. (2018) The microbial nitrogen-cycling network. *Nature Reviews. Microbiology*, 16, 263–276.

Letzel, A.-C., Li, J., Amos, G.C.A., Millán-Aguiñaga, N., Ginigini, J., Abdelmohsen, U.R. et al. (2017) Genomic insights into specialized metabolism in the marine actinomycete *Salinispora*. *Environmental Microbiology*, 19, 3660–3673.

Lewin, G.R., Carlos, C., Chevrette, M.G., Horn, H.A., McDonald, B.R., Stankey, R.J. et al. (2016) Evolution and ecology of Actinobacteria and their bioenergy applications. *Annual Review of Microbiology*, 70, 235–254.

Li, F., Chen, D., Lu, S., Yang, G., Zhang, X., Chen, Z. et al. (2018) Anti-influenza a viral butenolide from *Streptomyces* sp. Smu03 inhabiting the intestine of *Elephas maximus*. *Viruses*, 10, 356.

Liu, Y., Deng, Z., Tan, H., Deng, Q. & Cao, L. (2014) Characterization of cattle fecal *Streptomyces* strains converting cellulose and hemicelluloses into reducing sugars. *Environmental Science and Pollution Research International*, 21, 6069–6075.

Liu, M. & Douthwaite, S. (2002) Activity of the ketolide telithromycin is refractory to Erm monomethylation of bacterial rRNA. *Antimicrobial Agents and Chemotherapy*, 46, 1629–1633.

Lloyd, K.G., Steen, A.D., Ladau, J., Yin, J. & Crosby, L. (2018) Phylogenetically novel uncultured microbial cells dominate earth microbiomes. *mSystems*, 3, e00055-18.

Ma, J., Lei, H., Chen, X., Bi, X., Jiang, Y., Han, L. et al. (2017) New anti-inflammatory metabolites produced by *Streptomyces violaceoruber* isolated from *Equus burchelli* feces. *Journal of Antibiotics (Tokyo)*, 70, 991–994.

Ma, L., Zhang, W., Liu, Z., Huang, Y., Zhang, Q., Tian, X. et al. (2021) Complete genome sequence of *Streptomyces* sp. SCSIO 03032 isolated from Indian Ocean sediment, producing diverse bioactive natural products. *Marine Genomics*, 55, 100803.

Meier-Kolthoff, J.P., Carbasse, J.S., Peinado-Olarte, R.L. & Goker, M. (2022) TYGS and LPSN: a database tandem for fast and reliable genome-based classification and nomenclature of prokaryotes. *Nucleic Acids Research*, 50, D801–D807.

Mendes, R., Garbeva, P. & Raaijmakers, J.M. (2013) The rhizosphere microbiome: significance of plant beneficial, plant pathogenic, and human pathogenic microorganisms. *FEMS Microbiology Reviews*, 37, 634–663.

Millan-Aguinaga, N., Soldatou, S., Brozio, S., Munnoch, J.T., Howe, J., Hoskisson, P.A. et al. (2019) Awakening ancient polar Actinobacteria: diversity, evolution and specialized metabolite potential. *Microbiology*, 165, 1169–1180.

Nikolskiy, P.A., Sulerzhitsky, L.D. & Pitulko, V.V. (2011) Last straw versus Blitzkrieg overkill: climate-driven changes in the Arctic Siberian mammoth population and the late Pleistocene extinction problem. *Quaternary Science Reviews*, 30, 2309–2328.

Sayed, A.M., Hassan, M.H.A., Alhadrami, H.A., Hassan, H.M., Goodfellow, M. & Rateb, M.E. (2020) Extreme environments: microbiology leading to specialized metabolites. *Journal of Applied Microbiology*, 128, 630–657.

Soldatou, S., Eldjarn, G.H., Ramsay, A., van der Hooft, J.J.J., Hughes, A.H., Rogers, S. et al. (2021) Comparative metabologenomics analysis of polar actinomycetes. *Marine Drugs*, 19, 103.

Stursova, M., Zifcakova, L., Leigh, M.B., Burgess, R. & Baldrian, P. (2012) Cellulose utilization in forest litter and soil: identification of bacterial and fungal decomposers. *FEMS Microbiology Ecology*, 80, 735–746.

Sunagawa, S., Coelho, L.P., Chaffron, S., Kultima, J.R., Labadie, K., Salazar, G. et al. (2015) Ocean plankton. Structure and function of the global ocean microbiome. *Science*, 348, 1261359.

Tremaroli, V. & Backhed, F. (2012) Functional interactions between the gut microbiota and host metabolism. *Nature*, 489, 242–249.

Van Bergeijk, D.A., Elsayed, S.S., Du, C., Nunez Santiagio, I., Roseboom, A., Zhang, L. et al. (2022) The ubiquitous catechol moiety elicits siderophore and angucycline production in *Streptomyces*. *Communications Chemistry*, 5, 14.

van Bergeijk, D.A., Terlouw, B.R., Medema, M.H. & van Wezel, G.P. (2020) Ecology and genomics of Actinobacteria: new concepts for natural product discovery. *Nature Reviews Microbiology*, 18, 546–558.

Walker, B.J., Abeel, T., Shea, T., Priest, M., Abouelliel, A., Sakthikumar, S. et al. (2014) Pilon: an integrated tool for comprehensive microbial variant detection and genome assembly improvement. *PLoS One*, 9, e112963.

Wang, M., Carver, J.J., Phelan, V.V., Sanchez, L.M., Garg, N., Peng, Y. et al. (2016) Sharing and community curation of mass spectrometry data with Global Natural Products Social Molecular Networking. *Nature Biotechnology*, 34, 828–837.

Wetterich, S., Rudaya, N., Kuznetsov, V., Maksimov, F., Opel, T., Meyer, H. et al. (2019) Ice complex formation on Bol'shoy Lyakhovsky Island (new Siberian Archipelago, east Siberian Arctic) since about 200 ka. *Quaternary Research*, 92, 530–548.

Wibowo, M.C., Yang, Z., Borry, M., Hubner, A., Huang, K.D., Tierney, B.T. et al. (2021) Reconstruction of ancient microbial genomes from the human gut. *Nature*, 594, 234–239.

Wick, R.R., Judd, L.M., Gorrie, C.L. & Holt, K.E. (2017) Unicycler: resolving bacterial genome assemblies from short and long sequencing reads. *PLoS Computational Biology*, 13, e1005595.

Zhang, Z., Du, C., de Barsy, F., Liem, M., Liakopoulos, A., van Wezel, G.P. et al. (2020) Antibiotic production in *Streptomyces* is organized by a division of labor through terminal genomic differentiation. *Science Advances*, 6, eaay5781.

Zhang, C., Xu, B., Lu, T. & Huang, Z. (2019) Metagenomic analysis of the fecal microbiomes of wild Asian elephants reveals microflora and enzymes that mainly digest hemicellulose. *Journal of Microbiology and Biotechnology*, 29, 1255–1265.

Zhu, H., Swierstra, J., Wu, C., Girard, G., Choi, Y.H., van Wamel, W. et al. (2014) Eliciting antibiotics active against the ESKAPE pathogens in a collection of actinomycetes isolated from mountain soils. *Microbiology*, 160, 1714–1725.

Ziemert, N., Lechner, A., Wietz, M., Millan-Aguinaga, N., Chavarria, K.L. & Jensen, P.R. (2014) Diversity and evolution of secondary metabolism in the marine actinomycete genus *Salinispora*. *Proceedings of the National Academy of Sciences of the United States of America*, 111, E1130–E1139.

Zipperer, A., Konnerth, M.C., Laux, C., Berscheid, A., Janek, D., Weidenmaier, C. et al. (2016) Human commensals producing a novel antibiotic impair pathogen colonization. *Nature*, 535, 511–516.

SUPPORTING INFORMATION

Additional supporting information can be found online in the Supporting Information section at the end of this article.

How to cite this article: van Bergeijk, D.A., Augustijn, H.E., Elsayed, S.S., Willemse, J., Carrión, V.J., Du, C. et al. (2024) Taxonomic and metabolic diversity of Actinomycetota isolated from faeces of a 28,000-year-old mammoth. *Environmental Microbiology*, 26(2), e16589. Available from: https://doi.org/10.1111/1462-2920.16589